# Nanofiller incorporated poly(vinylidene fluoride–hexafluoropropylene) (PVdF–HFP) composite electrolytes for lithium batteries

A. Manuel Stephan [a,1], Kee Suk Nahm [a,*], T. Prem Kumar [b],
M. Anbu Kulandainathan [b], G. Ravi [c], J. Wilson [c]

[a] *School of Chemical Engineering and Technology, Chonbuk National University, Chonju 561-756, South Korea*
[b] *Central Electrochemical Research Institute, Karaikudi 630006, India*
[c] *Department of Physics, Alagappa University, Karaikudi 630003, India*

## Abstract

Composite polymer electrolyte (CPE) membranes, comprising poly(vinylidene fluoride–hexafluoropropylene) (PVdF–HFP), aluminum oxyhydroxide ($AlO[OH]_n$) of two different sizes 7 $\mu$m/14 nm and $LiN(C_2F_5SO_2)_2$ as the lithium salt were prepared using a solution casting technique. The prepared membranes were subjected to XRD, impedance spectroscopy, compatibility and transport number studies. Also Li $Cr_{0.01}Mn_{1.99}O_4$/CPE/Li cells were assembled and their charge–discharge profiles made at 70 °C. The incorporation of nanofiller greatly enhanced the ionic conductivity and the compatibility of the composite polymer electrolyte. The film which possesses a nanosized filler offered better electrochemical properties than a film with micron sized fillers. The results are discussed based on Lewis acid–base theory.
© 2005 Elsevier B.V. All rights reserved.

*Keywords:* Composite polymer electrolyte; Ionic conductivity; Compatibility: Lewis acid–base theory

## 1. Introduction

Very recently, studies reveal, that composite polymer electrolytes can alone offer a lithium battery with reliability and improved safety [1–4]. Solid polymer electrolytes derived from Li salt complexes with inorganic oxides such as $TiO_2$ and $Al_2O_3$ have been studied previously [5–11]. On the other hand, only a very few studies have been made on other polymer hosts such as poly(acrylonitrile) (PAN) [12], poly(methyl methacrylate) (PMMA) [13] and blended polymeric systems [14,15]. Composite polymer electrolytes based on poly(vinylidene fluoride–hexafluoropropylene) (PVdF–HFP) as a host have increasingly being investigated. This polymer host has some appealing properties. This PVdF–HFP itself has a high dielectric constant, $\varepsilon = 8.4$ that facilitates a higher concentration of charge carriers, and also comprises both an amorphous and a crystalline phase; the amorphous phase of the polymer assists

higher ionic conduction whereas the crystalline phase acts as a mechanical support for the polymer electrolyte. According to Scrosati and co-workers [1,2] and Wieczorek et al. [7] the Lewis acid–base interaction plays a vital role in the enhancement of the ionic conductivity of the composite polymer electrolytes. Moreover, in the present study, the filler, $AlO[OH]_n$ a basic substance, has not been investigated as a filler. Hence, an attempt was made to study the effect of the filler in different particle sizes on ionic conductivity and the compatibility with the composite polymer electrolytes and the results are described herein.

## 2. Experimental procedure

Poly(vinylidene fluoride–hexafluoro propylene) (Kynar, Japan) and lithium bis perfluorosulfonyl imide ($LiN(C_2F_5SO_2)_2$) were dried under vacuum at 90 °C for 12 h before use. The inert fillers, $AlO[OH]_n$ with different particle sizes 7 $\mu$m and 14 nm were also dried at 120 °C for 12 h before use. The preparation of a nanocomposite electrolyte involved the dispersion of the selected inert filler and a $LiN(C_2F_5SO_2)_2$ salt in anhydrous tetrahydrofuran (THF), followed by the addition of PVdF–HFP of different concentrations is depicted in Table 1 and the result-

---

Table 1
The composition of the polymer, lithium salt, filler content and transport number of the membranes prepared with different sizes of the fillers

| Sample | Polymer (wt.%) | Li salt (wt.%) | Filler (wt.%) | Transport number (Li+) of samples with | |
| --- | --- | --- | --- | --- | --- |
| | | | | (μm) | nm sized |
| S1 | 95 | 5 | 0 | 0.30 | 0.35 |
| S2 | 92.5 | 5 | 2.5 | 0.40 | 0.45 |
| S3 | 90 | 5 | 5.0 | 0.45 | 0.47 |
| S4 | 87.5 | 5 | 7.5 | 0.50 | 0.54 |
| S5 | 85 | 5 | 10.0 | 0.56 | 0.60 |
| S6 | 82.5 | 5 | 12.5 | 0.52 | 0.59 |
| S7 | 80 | 5 | 15.0 | 0.52 | 0.58 |
| S8 | 77.5 | 5 | 17.5 | 0.51 | 0.58 |

ing solution was cast to make a film in an argon atmosphere. The solvent was allowed to evaporate and the composite film had an average thickness of 30–50 μm. This procedure yielded homogenous and mechanically strong membranes, which were dried under vacuum at 80 °C for 24 h.

The prepared films were sandwiched between the two stainless steel discs of diameter 1 cm and the ionic conductivity of the membranes was measured using an electrochemical impedance analyzer (IM6-Bio Analytical Systems, USA) in the 50 mHz to 100 kHz frequency range at various temperatures viz., 0, 15, 30, 40, 50, 60, 70 and 80 °C. The values of $T_{Li}^+$ were measured by imposing a dc polarization pulse on a cell of the lithium-composite polymer electrolyte–lithium type and by following the time evolution of the resulting current flow using the expression [16,17].

$$Li^+ = \frac{I_s(V - I_0 R_0)}{I_0(V - I_s R_s)} \tag{1}$$

This method consists of measuring the ac impedance and current loss by dc chronoamperometry, respectively. The resistance and the current across a symmetrical Li/CPE/Li cell were polarized by a dc voltage pulse, $V$. In the present study the dc voltage pulse applied to the cell was 10 mV. The measurements were taken at the initial time of the applied dc voltage pulse ($t = t_0$, $R = R_0$, $l = l_0$) and under steady state conditions ($t = t_s$, $R = R_s$, $l = l_s$).

The compatibility of the Li/CPE/Li symmetric cells was investigated by studying the time dependence of the impedance of the systems in the open circuit condition at 70 °C. In the present study sample, S5 was used as it exhibited maximum ionic conductivity. The LiCr$_{0.01}$Mn$_{1.99}$O$_4$/CPE/Li cells were assembled using the procedure as reported elsewhere. The structural property of the nanocrystalline LiMn$_2$O$_4$ cathode material has already been reported by one of the authors [18].

## 3. Results and discussion

### 3.1. XRD analysis

Fig. 1a and b display the XRD patterns of PVdF–HFP polymer and PVdF–HFP + AlO[OH]$_n$ (of nanosized) + LiN(C$_2$F$_5$SO$_2$)$_2$ composite polymer electrolyte membranes, respectively. An exactly similar peak was observed for the films with micron sized filler (not shown in the figure). The peaks

at $2\theta = 18.2$, 20, 26.6 and 38, correspond to the (1 0 0) (0 2 0), (1 1 0) and (0 2 1) crystalline peaks of PVdF. This confirms the partial crystallization of PVdF units in the copolymer and gives a semi-crystalline structure of PVdF–HFP [19]. The crystallinity of the polymer has been considerably decreased upon the addition of the inert filler and lithium salt. It is quite obvious from the Fig. 1b that, the intensity of the crystalline peaks decreases and broadens. This reduction in crystallinity upon the addition of inert filler is attributed to small particles of inert filler, which changes the chain re-organization and facilitates higher ionic conduction [7]. These results are also in accordance with those reported for TiO$_2$ incorporated PMMA/PEGDA blend composite electrolyte system [14] and PAN–LiClO$_4$–α–Al$_2$O$_3$ composite system [13].

### 3.2. Ionic conductivity

The temperature dependence of polymer electrolyte membranes comprising PVdF–HFP–AlO[OH]$_n$ (micron sized) + LiN(C$_2$F$_5$SO$_2$)$_2$ and PVdF–HFP–AlO[OH]$_n$ (nano-sized) + LiN(C$_2$F$_5$SO$_2$)$_2$ as a function of filler content of different particles size is shown in Fig. 2a and b, respectively. The best conductivities of the composite polymer electrolytes at 30, 50 and 70 °C are depicted in Table 2. It is quite obvious from both figures that the ionic conductivity of the composite polymer electrolyte increases with the increase of temperature
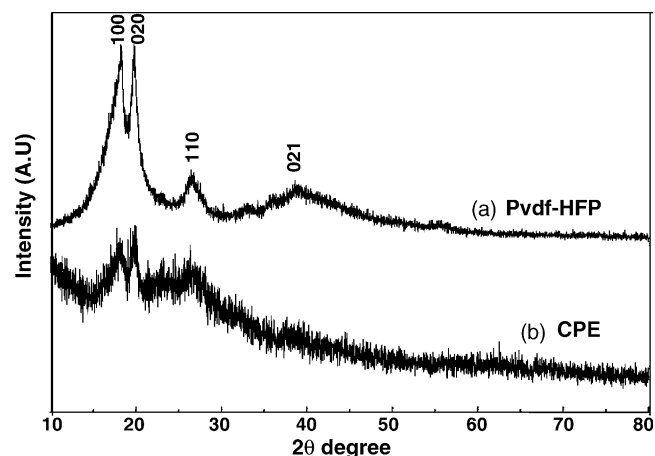


Fig. 1. XRD pattern of (a) PVdF–HFP + LiN(C$_2$F$_5$SO$_2$)$_2$; (b) PVdF–HFP + AlO[OH]$_n$ + LiN(C$_2$F$_5$SO$_2$)$_2$.
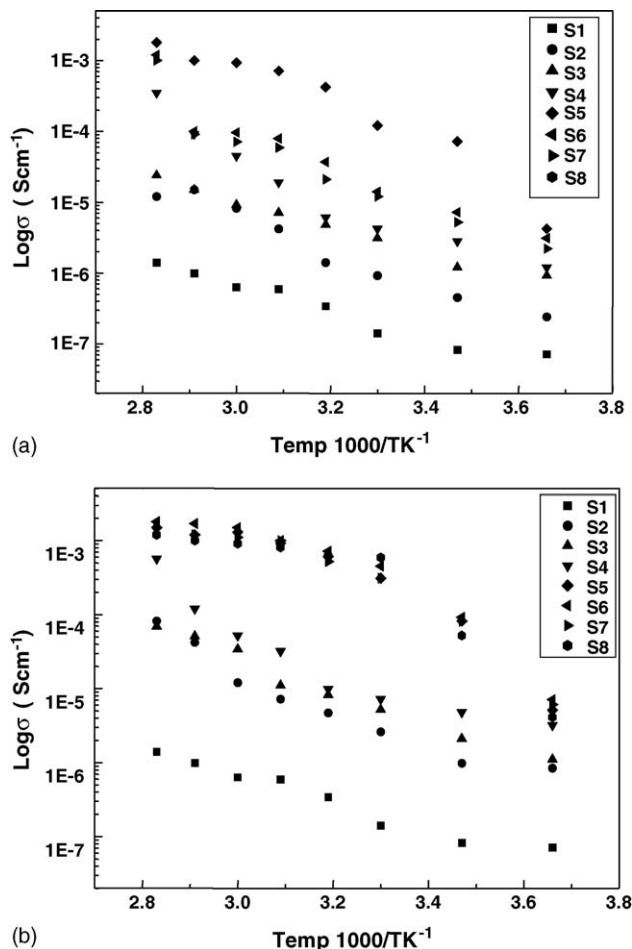
Fig. 2. (a) The temperature dependence of ionic conductivity of the composite polymer electrolyte of different filler contents (micron sized); (b) the temperature dependence of ionic conductivity of the composite polymer electrolyte of different filler contents (nanometer sized).

and also increases with the increase of filler content [20]. The ionic conductivity of the polymer membrane has considerably been increased by one order of magnitude upon the addition of filler in the polymer host. The ionic conductivity also increases with the increase of filler content up to 10 wt.% and then decreases with the increase of filler content. These results are in accordance with those reported earlier in which $Al_2O_3$ was used as filler in PEO-based electrolytes [21]. As commonly found in composite materials, the conductivity is not a linear function of the filler concentration. At low concentration levels the diffusion effect which, tends to depress the conductivity, is effectively opposed by the specific interactions of the ceramic surfaces, which promote fast ion transport. Hence, an

Table 2
The conductivities of the best electrolytes at 25, 50 and 75 °C

| S. no. | Sample composition | 30 °C S cm$^{-1}$ | 50 °C S cm$^{-1}$ | 75 °C S cm$^{-1}$ |
|--------|--------------------|----------------|----------------|----------------|
| 1. | S5 with filler of micron size | $1.2 \times 10^{-4}$ | $7.4 \times 10^{-4}$ | $1.0 \times 10^{-3}$ |
| 2. | S5 with filler of nanosize | $3.1 \times 10^{-4}$ | $9.2 \times 10^{-4}$ | $1.3 \times 10^{-3}$ |

apparent enhancement in conductivity is seen in both cases. At higher filler content, the dilution effect predominates and the conductivity is lowered. On the other hand, when the concentration of the filler was increased the dilution effect predominates and the conductivity decreases [21]. Thus, the maximum conductivity is achieved only in the concentration region of 8–10 wt.%. According to Scrosati and co-workers [2] from their NMR studies, the local dynamics of the lithium ions, in particular lithium mobility, is not changed by the filler which supports the idea that the enhancement of conductivity by adding a filler is caused by stabilizing and increasing the fraction of amorphous phase. Our XRD result also substantiates this point. However, indeed, this point does not hold good solely for the enhancement of conductivity where the polymer has an amorphous phase by its own nature. According to Scrosati and co-workers [1], the Lewis acid groups of the added inert filler may compete with the Lewis acid lithium cations for the formation of complexes with the PEO chains as well as the anions of the added lithium salt. Subsequently, this results in structural modifications of the filler surfaces, due to the specific actions of the polar surface groups of the inorganic filler. Although we do not have spectroscopic evidence, it is likely that the Li$^+$ complexes with the polymer through the highly reactive fluorine. The Lewis acid–base interaction centers with the electrolytic species, thus lowering the ionic coupling and promotes the salt dissociation via a sort of "ion-filler complex" formation. In the present study, the filler, AlO[OH]$_n$, which has a basic center can react with the Lewis acid centers of the polymer chain and these interactions lead to the reduction in the crystallinity of the polymer host. Indeed, this effect could be the reason for the observed enhancement in the ionic conductivity for both systems studied [7].

### 3.3. Compatibility studies

Although, the specific capacity of lithium metal is 3, 800 mAh g$^{-1}$ whereas that of carbon is 372 mAh g$^{-1}$ with a composition of LiC$_6$, the cycle life of lithium metal secondary cells is very short due to the low cycling efficiency of lithium metal anode as it reacts with both aprotic and protic solvents at its surface. Many reasons have been offered for this poor cycling, which, include electrochemical reactions between the anode and the electrolyte and loss of electronic contact between the electrode and dentritic lithium. In the polymer electrolyte systems, on the other hand, a resistive layer covers the lithium and the resistance of this layer grows with time, which can reach values over 10 K $\Omega$ cm$^{-2}$ [22]. Aurbach et al. [23] made a systematic study on the electrochemical processes of lithium electrodes and their surface chemistry, morphology and performance of lithium metal anodes for practical lithium rechargeable batteries. A similar study was reported by Matsuda et al. [24] where the authors studied the interfacial properties of lithium–organic electrolyte interface with inorganic and organic additives. The nature of this layer depends mainly on the purity and composition of the electrolyte. This interfacial resistance plays a crucial role in determining their properties, which include shelf life, safety and lithium deposition and dissolution efficiency and cycle life

Fig. 3. The variation of interfacial resistance "$R_i$" as a function of time for the Li/CPE/Li cell kept under open circuit condition at 70 °C. (■) PVdF–HFP + LiN($C_2F_5SO_2$)$_2$; (●) PVdF–HFP + AlO[OH]$_n$ + LiN($C_2F_5SO_2$)$_2$; (▼) PVdF–HFP–AlO[OH]$_n$ + LiN($C_2F_5SO_2$)$_2$.



Fig. 4. The schematic representation of composite polymer electrolytes with the inert filler of different sizes (adopted ref. [24]). (a) Particle with micron sized; (b) particle with nanosized.

[26]. As is well known, uncontrolled passivation phenomena affect the lithium electrode and thus the entire battery system and may lead to serious safety hazards eventually. Therefore, the criteria for the selection of a proper battery electrolyte must be based not only on fast transport properties but also, and perhaps principally, on favorable interfacial properties [26,27]. In the present study, the compatibility studies have been examined with proper attention to PVdF–HFP composite membranes as described in Section 2. Also the sample S5 was examined as this composition was found to be optimal in ionic conductivity. Table 2 shows the conductivity of the sample S5, at 30, 50 and 75 °C.

Fig. 3 displays the variation of interfacial resistance "$R_i$" as a function of time for the Li/CPE/Li symmetric cells kept on open circuit condition at 70 °C. As described by Abraham and co-workers [25], the interfacial resistance can be measured from the Cole–Cole impedance plots (not shown in the figure) in which the large semi-circles represent a parallel combination of resistance ($R_{film}$) and capacitance associated with the passivation film on the Li electrode. A small semicircle is due to the charge transfer resistance in parallel with the double layer capacitance. The intercept of the large semi-circle at high frequency on the $Z$-axis is mostly associated with the interfacial resistance "$R_i$" of the system. It is observed, from the figure that the composite polymer electrolyte containing nanosized filler is more compatible when lithium metal was used as the anode. However, on the other hand the film with a micron sized filler exhibits slightly higher interfacial resistance values. Also the PVdF–HFP co-polymer reacts with lithium at ambient and elevated temperatures. The growth of the interfacial resistance does not follow a regular trend for all the samples studied. After 160 h the resistance values do not change much. This may be attributed by assuming that the morphology of the passivation films changes with time to finally acquire a non-compact, possibly porous structure [17]. Furthermore, it is quite obvious from the figure that the interfacial resistance of the polymer host has considerably been reduced upon the incorporation of the inert filler (lower than the filler-free membrane). Interestingly, the presence of the hydroxyl group in the filler, which could react with metallic lithium, does not seem to have influenced the interfacial resistance. It is however, possible that the filler particles being covered with a polymer layer is not accessible for interaction with lithium.
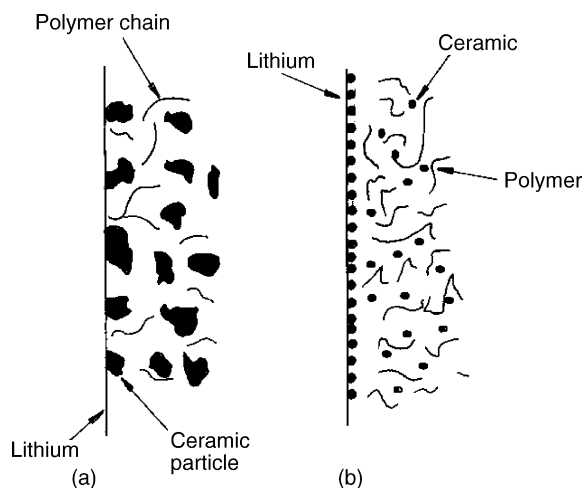
According to Kumar and Scanlon [4], nanosized inert fillers are more compatible than fillers which are micron sized. As depicted in Fig. 4, the inert particles depending upon the volume fraction would tend to minimize the area of the lithium electrode exposed to polymers containing O, OH-species and thus reduce the passivation process. It is also foreseeable that smaller size particles for a similar volume fraction of the ceramic phase would impart an improved performance as compared to larger size particles because they will cover more surface area [4]. The formation of an insulated layer of ceramic particles at the electrode surface is probable at a higher volume fraction of a passive ceramic phase. This insulating layer will impede electrode reactions. This may very well have happened when an excessive amount of the passive ceramic phase was introduced into the polymer matrix.

### 3.4. Transference number

In order to substantiate the conductivity results further, we have measured the Li⁺ transference number, $t_{Li^+}$, for all the samples and these are displayed in Table 1. This table reports the results in terms of numerical values of $t_{Li^+}$. The transference number values may equally be affected by the interfacial properties with lithium metal anode also [28]. An apparent increase in the transference number, $t_{Li^+}$ (Table 1) is observed when passing from the filler-free to the filler incorporated composite electrolytes. More interestingly, the transference number of the nanofiller incorporating composite polymer electrolytes exhibits higher values than the electrolytes with micron sized fillers which, further supports the ionic conductivity results.
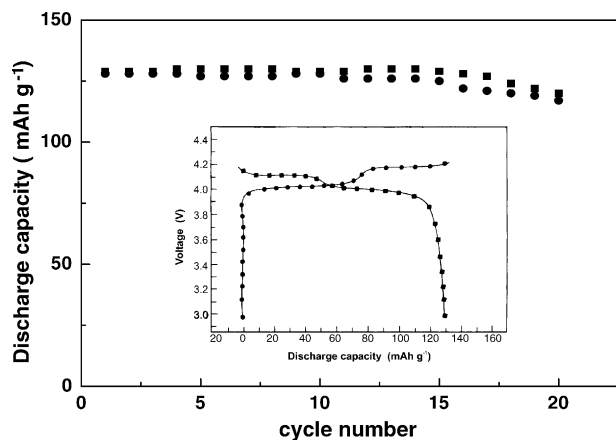
Fig. 5. The cycling behavior of Li LiCr$_{0.01}$Mn$_{1.99}$O$_4$ O$_4$/CPE/Li cells at 70 °C. (●) The polymer cell composed of LiCr$_{0.01}$Mn$_{1.99}$O$_4$/PVdF–HFP–AlO[OH]$_n$ 10% (micron sized)–LiN(C$_2$F$_5$SO$_2$)$_2$/Li and (■) LiCr$_{0.01}$Mn$_{1.99}$O$_4$/PVdF–HFP–AlO[OH]$_n$ 10% (nm sized)–LiN(C$_2$F$_5$SO$_2$)$_2$/Li. Inset show the first charge–discharge profile of LiCr$_{0.01}$Mn$_{1.99}$O$_4$/PVdF–HFP–AlO[OH]$_n$ 10% (nm sized)–LiN(C$_2$F$_5$SO$_2$)$_2$/Li cell at 70 °C.

## 3.5. Charge–discharge studies

Fig. 5 demonstrates the charge–discharge behavior of LiCr$_{0.01}$Mn$_{1.99}$O$_4$/PVdF–HFP–AlO[OH]$_n$ 10% (micron sized)–LiN(C$_2$F$_5$SO$_2$)$_2$/Li and LiCr$_{0.01}$Mn$_{1.99}$O$_4$/PVdF–HFP–AlO[OH]$_n$ 10% (nm sized)–LiN(C$_2$F$_5$SO$_2$)$_2$/Li cells at 70 °C. In the present study, the sample S5 has been employed as it was found to be optimal in ionic conductivity and from compatibility points of view. The lower and upper cut-off voltage of the cell was fixed as 2.8 and 4.2 V, respectively for fear of decomposition of the electrolyte. The cells were cycled at the 0.1C rate. The polymer cell composed of LiCr$_{0.01}$Mn$_{1.99}$O$_4$/PVdF–HFP–AlO[OH]$_n$ 10% (micron sized)–LiN(C$_2$F$_5$SO$_2$)$_2$/Li and LiCr$_{0.01}$Mn$_{1.99}$O$_4$/PVdF–HFP–AlO[OH]$_n$ 10% (nm sized)–LiN(C$_2$F$_5$SO$_2$)$_2$/Li delivered an initial discharge capacity of 128 and 129 mAh g$^{-1}$ and 120 and 117 mAh g$^{-1}$ after 20 cycles and the fade in capacity per cycle of the cells is 0.30 and 0.35 mAh g$^{-1}$, respectively. The cell which possess the membrane with micron sized fillers undergoes a slightly higher fade in capacity after 15 cycles and is attributed to high interfacial resistance of the system, Li/PVdF–HFP–AlO[OH]$_n$ 10% –LiN(C$_2$F$_5$SO$_2$)$_2$/Li as depicted in Fig. 3. A similar observation has reported by Yamamoto et al. [9] for PEO–LiBF$_4$–BaTiO$_3$ systems. It is possible that interactions between the lithium metal anode and the hydroxyl group in the filler could adversely influence the cyclability of the cell, although our studies on the compatibility of the CPE's with lithium do not support this argument. However, it is likely that during the dynamic changes occurring during the charge–discharge processes, lithium filler reactions could be initiated. The structural characteristics and composition of the cathode materials also play a vital role one the capacity of the cell. The fade in capacity of the systems may also be attributed to the Jahn–Teller distortion of the cathode material, LiCr$_{0.01}$Mn$_{1.99}$O$_4$ when operated below 3.5 V and also the operation of the cell at higher temperatures especially above 50 °C [29–32].

## 4. Conclusions

In the present study, the PVdF–HFP composite polymer electrolytes incorporating AlO[OH]$_n$ as an inert filler of two different particle sizes and LiN(C$_2$F$_5$SO$_2$)$_2$ as the lithium salt were prepared and electrochemical studies have been made. The incorporation of the inert filler not only reduces the crystallinity of the polymer host and acts as 'solid plasticizer' capable of enhancing the transport properties but also provides a better interfacial property towards a lithium metal anode. The cycling behavior of the LiCr$_{0.01}$Mn$_{1.99}$O$_4$/CPE/Li cells shows convincing results at elevated temperatures and may be employed as a separator for lithium polymer batteries for hybrid electric vehicle applications.

## References

[1] F. Croce, L. Perci, B. Scrosati, F. Serraino-Fiory, E. Plichta, M.A. Hendrickson, Electrochim. Acta 46 (2001) 2457–2461.
[2] G.B. Appetecchi, F. Croce, L. Persi, F. Ronci, B. Scrosati, Electrochim. Acta 45 (2000) 1481–1490.
[3] B. Kumar, L. Scanlon, R. Marsh, R. Mason, R. Higgins, R. Baldwin, Electrochim. Acta 46 (2001) 1515–1521.
[4] B. Kumar, L.G. Scanlon, J. Power Sources 52 (1994) 261–268.
[5] F. Croce, G.B. Appetecchi, L. Perci, B. Scrosati, Nature 394 (1998) 456–458.
[6] W. Wieczorek, A. Zalewska, D. Raducha, Z. Florjanczyk, J.R. Stevens, A. Ferry, P. Jacobsson, Macromolecules 29 (1996) 143–155.
[7] W. Wieczorek, J.R. Steven, Z. Florjanczyk, Solid State Ionics 85 (1996) 67–72.
[8] Q. Li, Y. Takeda, N. Imanish, J. Yang, J.K. Sun, J. Power Sources 97–98 (2001) 795–797.
[9] Q. Li, N. Imanishi, A. Hirano, Y. Takeda, O. Yamamoto, J. Power Sources 110 (2002) 38–45.
[10] Q. Li, T. Itoh, N. Imanishi, A. Hirano, Y. Takeda, O. Yamamoto, Solid State Ionics 159 (2003) 97–109.
[11] G.B. Appetecchi, J. Hassoun, J.B. Scrosati, F. Croce, F. Cassel, M. Salomon, J. Power Sources 124 (2003) 246–253.
[12] Z. Wang, H. Huang, L. Chen, Electrochem. Solid State Lett. 6 (2003) E40–E44.
[13] H.S. Kim, K.S. Kum, W. Cho II, B. Woncho, W.H. Rhee, J. Power Sources 124 (2003) 221–224.
[14] S.T. Joy Kumar, S.V. Bhat, J. Power Sources 129 (2004) 280–287.
[15] D. Noto, V. Zago, J. Electrochem. Soc. 151 (2004) A216–A223.
[16] P.G. Bruce, C.A. Vincent, J. Electroanal. Chem. 225 (1987) 1–17.
[17] G.B. Appetecchi, F. Croce, B. Scrosati, Electrochim. Acta 40 (1995) 991–997.
[18] A. Manuel Stephan, Dale-Teeters Electrochim. Acta 48 (2003) 2143–2148.
[19] D. Saika, A. Kumar, Electrochim. Acta 49 (2004) 2581–2589.
[20] Y. Liu, J.Y. Lee, L. Hong, J. Power Sources 129 (2004) 303–311.
[21] X. Qian, N. Gu, Z. Cheng, X. Yang, E. Wang, S. Dong, Electrochim. Acta 46 (2001) 1829–1836.
[22] D. Fauteax, J. Electrochem Soc. Proc. 94–28 (1994) 379–384.
[23] D. Aurbach, I. Weissman, H. Yamin, E. Elster, J. Electrochem. Soc. 145 (1998) 1421–1426.
[24] Y. Matsuda, M. Ishikawa, S. Yoshitake, M. Morita, J. Power Sources 54 (1995) 301–305.
[25] Z. Jiang, B. Carroll, K.M. Abraham, Electrochim. Acta 42 (1997) 2667–2677.
[26] J. Kuratomi, T. Iguchi, T. Bando, Y. Aihara, T. Ono, K. Kuwana, J. Power Sources 97–98 (2001) 801–803.

[27] K. Kanamura, H. Tamura, S. Shiraishi, Z. Takehara, J. Electrochem. Soc. 142 (1995) 340–347.

[28] J. Evans, C.A. Vincent, P.G. Bruce, Polymer 28 (1987) 2325–2328.

[29] B.J. Hwang, R. Santhanam, J. Power Sources 108 (2002) 250–255.

[30] G.T.K. Fey, C.Z. Lu, T. Prem Kumar, J. Power Sources 115 (2003) 332–345.

[31] D.H. Jiang, J.Y. Shin, S.M. Oh, J. Electrochem. Soc. 143 (1996) 2204–2211.

[32] Y. Xia, Y. Zhou, M. Yoshio, J. Electrochem. Soc. 144 (1997) 2593–2600.